Tetanus Toxin and Botulinum Toxin A Utilize Unique Mechanisms To Enter Neurons of the Central Nervous System

Faith C. Blum, Chen Chen,* Abby R. Kroken, and Joseph T. Barbieri

Medical College of Wisconsin, Microbiology and Molecular Genetics, Milwaukee, Wisconsin, USA

Botulinum neurotoxins (BoNTs) and tetanus neurotoxin (TeNT) are the most toxic proteins for humans. While BoNTs cause flaccid paralysis, TeNT causes spastic paralysis. Characterized BoNT serotypes enter neurons upon binding dual receptors, a ganglioside and a neuron-specific protein, either synaptic vesicle protein 2 (SV2) or synaptotagmin, while TeNT enters upon binding gangliosides as dual receptors. Recently, TeNT was reported to enter central nervous system (CNS) neurons upon synaptic vesicle cycling that was mediated by the direct binding to SV2, implying that TeNT and BoNT utilize common mechanisms to enter CNS neurons. This prompted an assessment of TeNT entry into CNS neurons, using the prototypic BoNT serotype A as a reference for SV2-mediated entry into synaptic vesicles, analyzing the heavy-chain receptor binding domain (HCR) of each toxin. Synaptic vesicle cycling stimulated the entry of HCR/A into neurons, while HCR/T entered neurons with similar levels of efficiency in depolarized and nondepolarized neurons. ImageJ analysis identified two populations of cell-associated HCR/T in synaptic vesicle cycling neurons, a major population which segregated from HCR/A and a minor population which colocalized with HCR/A. HCR/T did not inhibit HCR/A entry into neurons in competition experiments and did not bind SV2, the protein receptor for BoNT/A. Intoxication experiments showed that TeNT efficiently cleaved VAMP2 in depolarized neurons and neurons blocked for synaptic vesicle cycling. These experiments demonstrate that TeNT enters neurons by two pathways, one independent of stimulated synaptic vesicle cycling and one by synaptic vesicles independent of SV2, showing that TeNT and BoNT/A enter neurons by unique mechanisms.

The clostridial neurotoxins (CNTs) are the most toxic proteins for humans and include category A agents, the botulinum neurotoxins (BoNTs) (19). CNT neuronal toxicity occurs by specific binding to neuronal receptors and cleavage of neuron-specific soluble *N*-ethylmaleimide-sensitive factor attachment protein receptor (SNARE) proteins. CNTs are synthesized as single-chain A-B toxins that are nicked to an N-terminal light-chain protease domain (LC) which remains associated with the C-terminal heavy chain (HC) by a disulfide bond (33). The HC comprises a translocation domain (HCT) and a receptor binding domain (HCR). The HCR is composed of an N-terminal subdomain (HCRN) and a C-terminal subdomain (HCRC). HCRN has not been assigned a function, while HCRC contains dual, host neuron-specific receptor binding pockets (27, 28, 35).

CNTs also include tetanus neurotoxin (TeNT), which shares ~35% amino acid identity and a conserved tertiary structure with BoNTs (24). Although BoNTs and TeNT cleave SNARE proteins, BoNTs elicit flaccid paralysis and TeNT elicits spastic paralysis due to differential trafficking within α-motor neurons. BoNTs are classified into seven serotypes (A to G). BoNT/A and BoNT/E cleave synaptosomal-associated protein of 25 kDa (SNAP25) (3, 4, 27, 36, 38); BoNT/B, BoNT/D, BoNT/F, BoNT/G, and TeNT cleave vesicle-associated membrane protein 2 (VAMP2, also referred to as synaptobrevin 2); and BoNT/C cleaves SNAP25 and syntaxin 1A (5, 17, 27, 29, 30, 35). The observation that TeNT and BoNT/B cleave VAMP2 at the same residue underscores the importance of intracellular trafficking as being responsible for their unique pathologies (12, 37).

Membrane depolarization stimulates the opening of Ca^{2+} channels and entry of extracellular Ca^{2+} into neurons, which drives synaptic vesicle (SV) exocytosis (42). Synaptotagmin binds intracellular Ca^{2+} and initiates migration of the SV to the plasma membrane, where fusion releases neurotransmitters into the synapse (42). The mechanism for SV cycling from the plasma membrane is complex: in addition to direct SV cycling, a rapid endosome pathway retrieves SV proteins from the plasma membrane (22).

BoNT/A entry into neurons follows the initial binding to ganglioside on the surface of α-motor neurons (26, 27). Upon fusion of SVs to the plasma membrane, BoNT/A binds a luminal domain of synaptic vesicle protein 2 (SV2) and is internalized upon SV cycling off the membrane (13). Acidification of the lumen of the SV stimulates HCT insertion into the SV membrane, which facilitates translocation of the LC into the cytosol (16). On α-motor neurons, TeNT binds receptors concentrated in lipid microdomains (21), which include polysialogangliosides. TeNT is endocytosed via a clathrin- and Rab5-mediated pathway and retrograde traffics within the lumen of neutral endosomes that are marked with Rab7 (20). TeNT is transcytosed to an interneuronal synapse by a mechanism that remains undefined, where TeNT binds and intoxicates neurons of the central nervous system (CNS), blocking the release of inhibitory neurotransmitters and eliciting spastic paralysis (39, 40). Recent studies reported that TeNT entered neurons of the CNS upon membrane depolarization (25, 43), through

a direct interaction with SV2 similar to that seen with BoNT/A (43). This prompted the current study to establish how TeNT enters CNS neurons, which identified two entry pathways utilized by TeNT. One pathway is independent of stimulated SV cycling, and the second pathway is mediated by SVs but is independent of a direct interaction with SV2, making it distinct from that of BoNT/A.

MATERIALS AND METHODS

Production and purification of BoNT/A and TeNT. TeNT was purchased from List Biological (CA). Production and purification of the receptor binding domain (FLAG-HCR/A) of BoNT/A (residues 870 to 1296) and FLAG-tagged or hemagglutinin (HA)-tagged HCR/T of TeNT (residues 865 to 1315) were performed as previously described (1, 9).

Rat cortical neuron cultures. Glass-bottomed 24-well plates (MatTek) or 12-well plates (Falcon) were incubated overnight at room temperature (RT) with poly-D-lysine (P0899; Sigma) (50 μg/ml of water, 0.5 ml/well for 24-well plates and 1 ml/well for 12-well plates). Plates were washed with cell-culture-grade water twice and incubated in complete neurobasal medium for at least 1 h at 37°C (0.5 ml for 24-well plates and 1 ml for 12-well plates) before neurons were plated. Rat E18 cortical neurons or rat E18 hippocampal neurons (BrainBits LLC) were cultured in neurobasal medium (catalog no. 21103; Invitrogen) supplemented with 0.5 mM Glutamax-I (catalog no. 35050; Invitrogen), 2% B27 supplement (catalog no. 17504; Invitrogen), and Primocin (InvivoGen). After 7 days, half of the medium was replenished. Neurons were used at day 10 to 14 postplating.

HCR/A and HCR/T binding to rat cortical neurons. Cortical neurons were incubated with 40 nM FLAG-HCR/T or FLAG-HCR/A for 1 h at 4°C in low potassium buffer (low K buffer: 15 mM HEPES, 145 mM NaCl, 5.6 mM KCl, 2.2 mM CaCl, 0.5 mM MgCl$_2$, pH 7.4) or under membrane depolarizing conditions with calcium (high K buffer: 15 mM HEPES, 95 mM NaCl, 56 mM KCl, 2.2 mM CaCl, 0.5 mM MgCl$_2$, pH 7.4) or without calcium (high K/EGTA buffer: 15 mM HEPES, 95 mM NaCl, 56 mM KCl, 0.5 mM MgCl$_2$, 0.2 mM EGTA, pH 7.4) and then washed with Dulbecco's phosphate-buffered saline (DPBS). Cells were collected in radioimmunoprecipitation assay (RIPA) buffer with mammalian protease inhibitors (Sigma), incubated for 5 min on ice, and centrifuged (16,000 × g, 3 min), and soluble material was subjected to SDS-PAGE and Western blotting. HCRs contained an N-terminal 3×FLAG epitope and were detected with horseradish peroxidase (HRP)-conjugated mouse anti-FLAG M2 antibody (final dilution of 1:20,000; Sigma). Alternatively, cells were processed for immunofluorescence (IF).

Immunofluorescence. Cells were fixed with 4% (wt/vol) paraformaldehyde in DPBS for 15 min at RT, washed twice with DPBS, and subjected to IF. Cells were incubated with Alexa 594-wheat germ agglutinin (WGA) (1:500 dilution, catalog no. I34406; Invitrogen) in PBS for 15 min at RT, washed, and fixed again with 4% (wt/vol) paraformaldehyde in DPBS for 15 min at RT. Cells were then permeabilized with 0.1% Triton X-100 in 4% formaldehyde in DPBS for 15 min at RT, incubated with 150 mM glycine in DPBS for 10 min at RT, washed with DPBS twice, and incubated in blocking solution (10% [vol/vol] normal goat serum, 2.5% [wt/vol] cold fish skin gelatin [Sigma], 0.1% Triton X-100, 0.05% Tween 20 in DPBS) for 1 h at RT. Following this incubation, cells were treated with primary antibody in antibody incubation solution (5% [vol/vol] normal goat serum, 1% [wt/vol] cold fish skin gelatin, 0.1% Triton X-100, 0.05% Tween 20 in DPBS) overnight at 4°C. Cells were washed 5 times with DPBS and incubated with goat or rat IgG Alexa-labeled secondary antibodies (Molecular Probes) in antibody incubation solution for 1 h at RT. Cells were washed 3 times, fixed with 4% paraformaldehyde in DPBS for 15 min at RT, and washed with DPBS. Mounting reagent Citifluor AF-3 (Electron Microscopy Sciences) was added, and images were captured with a Nikon TE2000 total internal reflection fluorescence (TIRF) microscope equipped with a CFI Plan Apo VC 100× oil, numerical-aperture (NA) 1.49 type objective using a Photometrics CoolSnap HQ2 camera.

Image analyses were performed using MetaMorph version 7.0, and figures were compiled using Photoshop CS (Adobe).

Entry and colocalization of HCR/A and HCR/T with intracellular marker proteins. Cortical neurons were incubated with 40 nM FLAG-HCR/A or FLAG-HCR/T or transferrin-Alexa 488 (5 μg/ml) for 5 min at 37°C in low K buffer or high K buffer and fixed as described above. FLAG or HA epitope-tagged HCRs were analyzed in this study. HCRs were probed with mouse anti-FLAG M2 antibody (1:15,000 dilution; Sigma) or rat anti-HA antibody (1:2,000 dilution; Roche), and marker proteins were probed with rabbit anti-Rab5 antibody (1:1,000 dilution; Abcam) and guinea pig or mouse anti-synaptophysin 1 antibody (1:2,000 dilution [SYSY 101002] or 1:1,000 dilution [SYSY 101011]). Bound primary antibodies were detected with goat anti-mouse IgG, donkey anti-rat IgG, goat anti-rabbit IgG, or goat anti-guinea pig IgG conjugated to Alexa 488, 561, or 633 (1:250 to 1:1,000 dilution; Invitrogen). Images were captured by TIRF microscopy. Intracellular colocalization measurements, determined as percentages, were performed using Metamorph version 7.0. Background (anti-FLAG and anti-HA antibody staining without added HCRs or Rab5 and synaptophysin staining without primary antibodies) was calculated using a median filter of 32 by 32 using Process: Median Filter. Background was subtracted from test images using Process: Arithmetic. For colocalization analysis, thresholds were set for test and background images and measured using Process: Measure Colocalization. Percent colocalization was defined as the area of colocalization between two markers divided by the area of one marker, multiplied by 100. Correlation coefficients were measured using WCIF-ImageJ version 1.37c. Pearson's (correlation) coefficients were calculated using the Manders Coefficients plugin. We have observed that segregated staining is demonstrated by a correlation coefficient below 0.3; dependent staining is a correlation coefficient above 0.6. Values between 0.3 and 0.6 have complex staining. Rat cortical neurons were also incubated with anti-synaptotagmin 1 Oyster 650 antibody, which recognizes a luminal epitope of synaptotagmin (1:400 dilution; SYSY 105311C5), in low K buffer, high K buffer, or high K/EGTA buffer for 5 min at 37°C. Cells were washed, fixed, and imaged for internalized antibody by TIRF microscopy as described above.

CNT cleavage of VAMP2 in rat cortical neurons. Rat cortical neurons were washed twice with DPBS and incubated with 40 nM TeNT in low K buffer, high K buffer, or high K/EGTA buffer for 20 min at 37°C. Cells were washed with DPBS and incubated in conditioned neurobasal medium for an additional 18 h. Cells were washed with DPBS prior to fixation and processed for immunofluorescence as described above. VAMP cleavage was assayed with mouse anti-VAMP2/synaptobrevin antibody (1:500 dilution; SYSY clone 69.1), which recognizes only intact VAMP2/synaptobrevin. Alternatively, rat cortical neurons were incubated with 1 nM BoNT/D in neurobasal medium for 18 h. Intoxicated and control neurons were washed twice with DPBS and incubated with HCR/A, HCR/T, or antisynaptotagmin, with time and buffer as indicated in the figure legends. Cells were washed with DPBS, fixed, and processed for immunofluorescence.

Immunoprecipitation. Synaptic vesicle lysate was prepared from rat brains (Pel-Freez Corp.) as described previously (1) and solubilized in 0.5% CHAPS {3-[(3-cholamidopropyl)-dimethylammonio]-1-propanesulfonate} or 0.5% Triton X-100 in 10 mM HEPES, pH 7.4, with mammalian protease inhibitors (Sigma-Aldrich). Five μg of HCR was added to 1 ml of buffer containing 10 μg synaptic vesicle lysate, and the mixture was incubated for 30 min at 4°C. Forty μl of M2 FLAG-agarose beads (Sigma-Aldrich) was blocked in 1% bovine serum albumin (BSA) and added to the HCR and synaptic vesicle mixture, which was incubated for 2 h at 4°C with gentle rotation. Beads were recovered by centrifugation and washed three times with 900 μl of HEPES buffer with detergent and protease inhibitors. Specific FLAG interactions were eluted with 150 μg FLAG peptide (Sigma-Aldrich) for 30 min. Soluble material was removed and analyzed by SDS-PAGE and Western blotting. Immunoprecipitations were probed for SV2A (mouse, 1:5,000 dilution), SV2B (rabbit, 1:500 dilution; SYSY 119102), SV2C (rabbit, 1:500 dilution; SYSY 119202), and
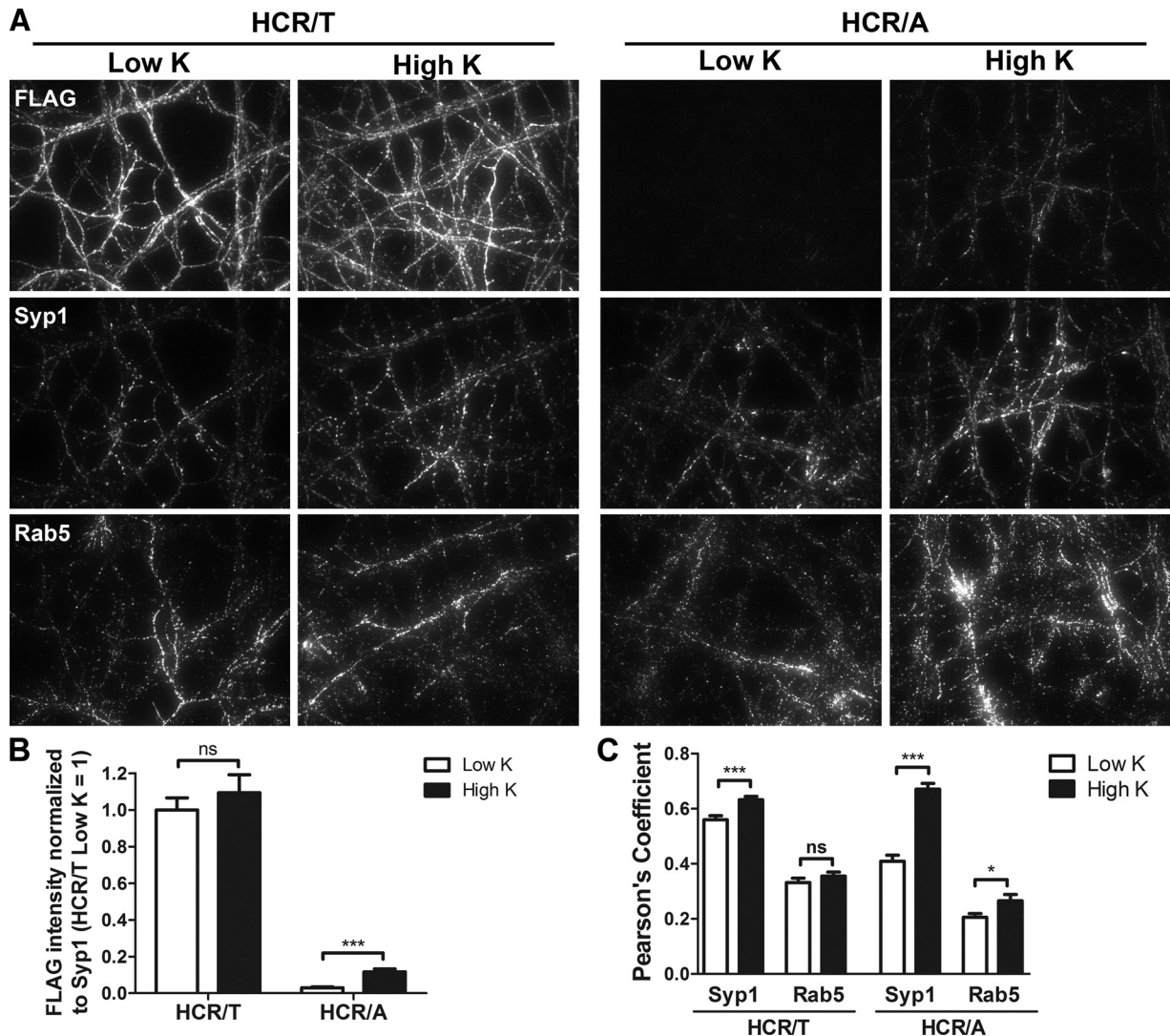
FIG 1 HCR/T and HCR/A entry into cortical neurons. FLAG-HCR/T or FLAG-HCR/A (40 nM) was incubated with rat cortical neurons in low K buffer or high K buffer for 5 min at 37°C. (A) IF was performed to detect HCRs, Rab5, and synaptophysin 1 (Syp1). (B) Six random fields were selected for IF intensity analysis. The IF ratio between anti-FLAG and antisynaptophysin was used as a marker for HCR/T and HCR/A internalization. (C) HCR colocalization with Syp1 or Rab5 was analyzed as described in Materials and Methods. Student's t test was performed. ns, not significant ($P > 0.05$); *, $P < 0.05$; ***, $P < 0.001$. Error bars indicate standard deviations.

FLAG. The SV2A monoclonal antibody developed by K. M. Buckley was obtained from the Developmental Studies Hybridoma Bank developed by the National Institute of Child Health and Human Development and maintained by the Department of Biological Sciences, University of Iowa (Iowa City, IA). Densitometry was performed with Alpha Imager software.

RESULTS

Entry of HCR/T and HCR/A into primary cortical neurons. Binding and entry into cortical neurons were monitored by total internal reflection fluorescence (TIRF) microscopy. TIRF microscopy facilitates measurements near the plasma membrane that are difficult to quantify by conventional microscopy due to the density of axons formed by cultured primary neurons. TIRF microscopy detects fluorescence within approximately 100 nm of the coverslip, largely eliminating signal from the cell body and focusing our study on axons and dendrites of the cultured neurons. SV

cycling was stimulated by incubating primary cortical, hippocampal, or spinal cord neurons in a high concentration of potassium with extracellular calcium (56 mM KCl with 2.2 mM CaCl). Toxin entry was measured by analyzing the epitope-tagged receptor binding domains of BoNT/A (HCR/A) and TeNT (HCR/T), which are nontoxic but retain the structure-function properties and compete with CNTs for entry into cells (9, 10, 33). The HCRs were tagged with FLAG or HA epitopes, which exhibit the same binding properties for all assays performed. BoNT/A enters neurons specifically through SVs, due to interactions with SV2 (13); we used the uptake of HCR/A as a control for SV cycling and as a marker for SVs which have fused to the plasma membrane.

At 4°C, HCR/T binding to primary neurons was readily detected, while HCR/A binding was near background levels (see Fig. S1 in the supplemental material). This indicated a difference in initial association of TeNT and BoNT/A with neurons. At 37°C,
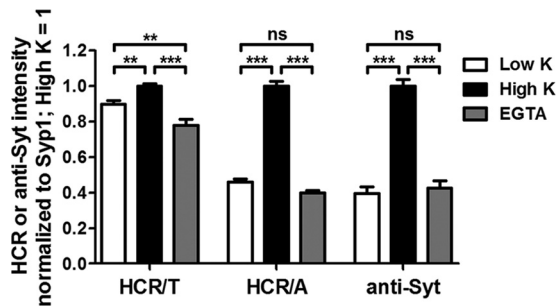
FIG 2 Calcium-dependent entry of HCR/A into cortical neurons. HA-HCR/T, HA-HCR/A, or anti-Syt1 antibody (40 nM) was incubated with rat cortical neurons in low K buffer or high K buffer containing 2.2 mM Ca^{2+}, or in high K buffer without Ca^{2+} and containing 0.2 mM EGTA, for 5 min at 37°C. IF analysis was performed using ImageJ, as described in Materials and Methods. For each set of signals, the high K signal was set to 1. One-way analysis of variance (ANOVA) was performed for the data set. ns, not significant ($P > 0.05$); **, $P < 0.01$; ***, $P < 0.001$. Error bars indicate standard deviations.

HCR/T bound depolarized and nondepolarized neurons (high or low extracellular potassium) with similar levels of intensity. In contrast, HCR/A binding to nondepolarized neurons was near background levels and was detectable in depolarized neurons (Fig. 1). HCR/T colocalized with synaptophysin (SV protein marker) in high K buffer and low K buffer, while the colocalization of HCR/A with synaptophysin was greater in high K buffer than in low K buffer. There was limited colocalization of HCR/T or HCR/A with Rab5, an endosome marker protein. Thus, HCR/T and HCR/A associate uniquely with neurons, but both do so through SV protein-specific entry pathways. Quantitation showed that in depolarized neurons there was ~20-fold more HCR/T cell bound than HCR/A and that the amount of HCR/T bound was dose dependent (see Fig. S2 in the supplemental material). Additional experiments indicated that HCR/A and HCR/T entered hippocampal and spinal cord neurons similarly to cortical neurons (data not shown). As cortical neurons are more abundant than either hippocampal or spinal cord neurons, experiments were continued with cortical neurons.

Calcium-dependent entry of HCR/T and HCR/A in neurons. Since SV cycling requires extracellular Ca^{2+}, experiments assessed Ca^{2+} dependency of HCR/T entry into neurons. HCR/A association with neurons was Ca^{2+} dependent and inhibited by EGTA (Fig. 2), as would be expected given the necessity for SV cycling in HCR/A entry (13). In contrast, HCR/T association with neurons was Ca^{2+} independent and not inhibited by EGTA (Fig. 2). Additional controls showed that the stimulation of SV cycling increased the cell association of anti synaptotagmin1 IgG (anti-Syt1 IgG), an antibody that binds to a luminal domain of synaptotagmin 1 that is surface exposed upon the fusion of SVs with the cell membrane; cell association of anti-Syt1 IgG was inhibited with EGTA.

Inhibition of SV cycling differentiates entry of HCR/A and HCR/T. Neurons were incubated with BoNT/D overnight to cleave intracellular VAMP2 and inhibit SV cycling (29) and then assayed for entry by HCR/A, HCR/T, or anti-Syt1 IgG. BoNT/D was used to inhibit SV cycling, since the amount of intracellular SNARE protein VAMP2 cleaved can be assessed by immunofluorescence. Overnight incubation with BoNT/D reduced intracellular VAMP2 to background levels (Fig. 3, top right) and eliminated
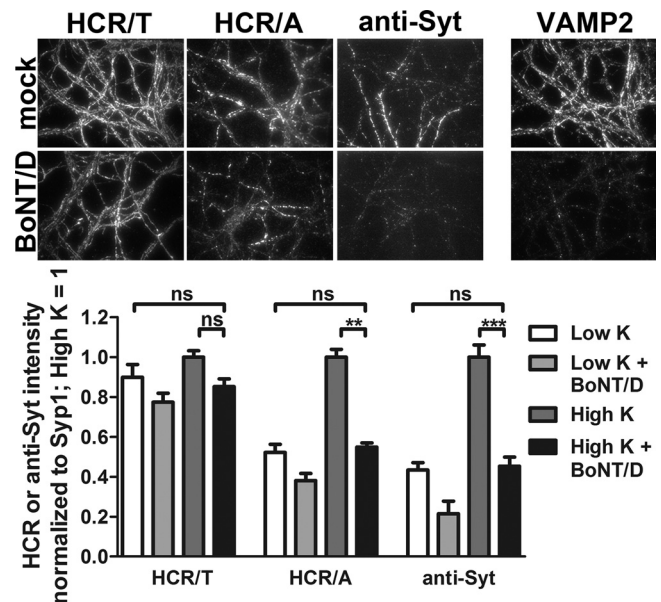
FIG 3 BoNT/D intoxication has a differential effect on HCR/A and HCR/T entry into neurons. BoNT/D (1 nM) was incubated with rat cortical neurons for 18 h. After being washed, neurons were incubated with 40 nM HA-HCR/T, HA-HCR/A, or Oyster 650 antisynaptotagmin antibody (anti-Syt, 1:400 dilution) for 5 min in low K buffer or high K buffer and then processed for IF. Representative images of indicated proteins after the 5-min incubation in high K buffer are shown. Relative intensities were normalized to the level for Syt; the high K signal was set to 1 within each data set. ns, not significant ($P > 0.05$); **, $P < 0.01$; ***, $P < 0.001$. Error bars indicate standard deviations.

SV cycling assessed by uptake of HCR/A and anti-Syt1 IgG (Fig. 3). HCR/T bound BoNT/D-intoxicated neurons with similar levels of efficiency in high K buffer and in low K buffer.

SV cycling stimulates entry of HCRs into SVs. To increase the resolution of the CNT entry into neurons, differentially epitope-labeled HCRs (HA-HCR/T and FLAG-HCR/A) were colocalized in neurons (Fig. 4). In SV cycling neurons, most HCR/T segregated from HCR/A. The pool of colocalized HCR/T and HCR/A constituted ~25% of the HCR/T signal and ~80% of the HCR/A signal. The different percentages of the colocalized HCRs are due to more HCR/T cell bound than HCR/A. ImageJ visualized three populations of cell-associated HCRs: cell-associated HCR/T that was segregated from HCR/A, the fraction of HCR/T that was colocalized with HCR/A, and HCR/A segregated from HCR/T (Fig. 5). This analysis showed that the majority of HCR/T associated with neurons independent of HCR/A, with a fraction of HCR/T which colocalized with HCR/A, presumably within SVs, and that little HCR/A was segregated from HCR/T. Controls show the resolution of ImageJ imaging, measuring the colocalization of two different epitopes within synaptophysin 1 and the segregation of transferrin and synaptophysin 1, which localize in different regions of neurons.

HCR/T does not compete with HCR/A entry into SVs. The observation that a fraction of HCR/T colocalized with HCR/A in SV cycling neurons prompted an experiment to determine if HCR/T competes with HCR/A for entry into SVs. In this experiment, the cell association of FLAG-HCR/A with neurons was competed with a 10-fold excess of HA-HCR/A or HA-HCR/T. Excess HA-HCR/A reduced the amount of cell-associated FLAG-
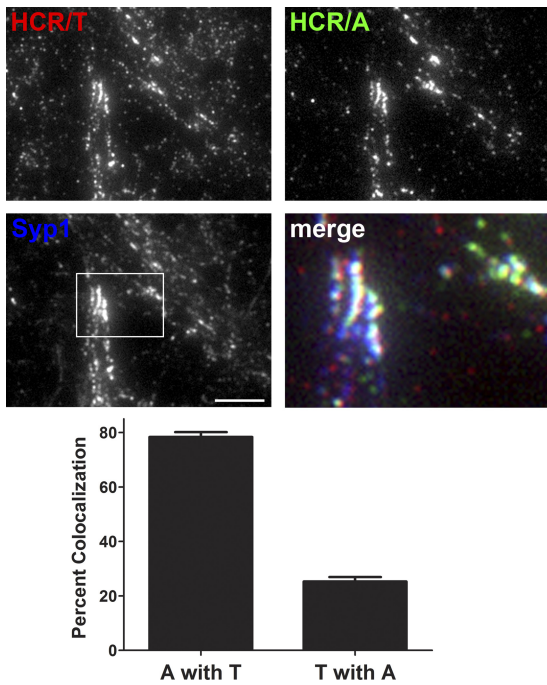
FIG 4 Partial colocalization of HCR/T and HCR/A in SVs of cortical neurons. HA-HCR/T or FLAG-HCR/A (40 nM) was incubated with rat cortical neurons in high K buffer for 5 min at 37°C. Neurons were fixed and stained with anti-HA (red), anti-FLAG (green), and anti-Syp (blue). Bar, 20 μm. Colocalization was determined as a percentage of FLAG-HCR/A (A) colocalized with HA-HCR/T (T) or HA-HCR/T colocalized with FLAG-HCR/A, using MetaMorph 7.0. Data were averaged from 10 independent fields. Error bars indicate standard deviations.
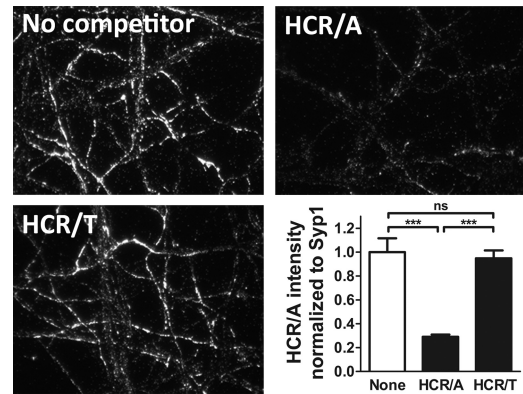
FIG 6 Competition of HCR/A and HCR/T for binding cortical neurons. FLAG-HCR/A (20 nM), alone (No competitor) or with 200 nM HA-HCR/A or 200 nM HA-HCR/T, was incubated with rat cortical neurons in high K buffer for 5 min at 37°C. Neurons were fixed and stained with anti-FLAG and anti-Syp. Intensity was analyzed by ImageJ. Shown is a representative data set from 3 independent replicates, with corresponding micrographs stained with anti-FLAG. ns, not significant ($P > 0.05$); ***, $P < 0.001$. Error bars indicate standard deviations.

HCR/A, but excess HA-HCR/T did not reduce the amount of cell-associated FLAG-HCR/A (Fig. 6). The lack of competition by HCR/T for HCR/A entry indicated that HCR/T and HCR/A utilize different mechanisms to enter neurons. The reciprocal experiment, a competition for HCR/T binding, was not performed, since HCR/T binding was not saturated in this assay. The self-competition of HCR/A is likely at the level of limited SV2 binding sites.
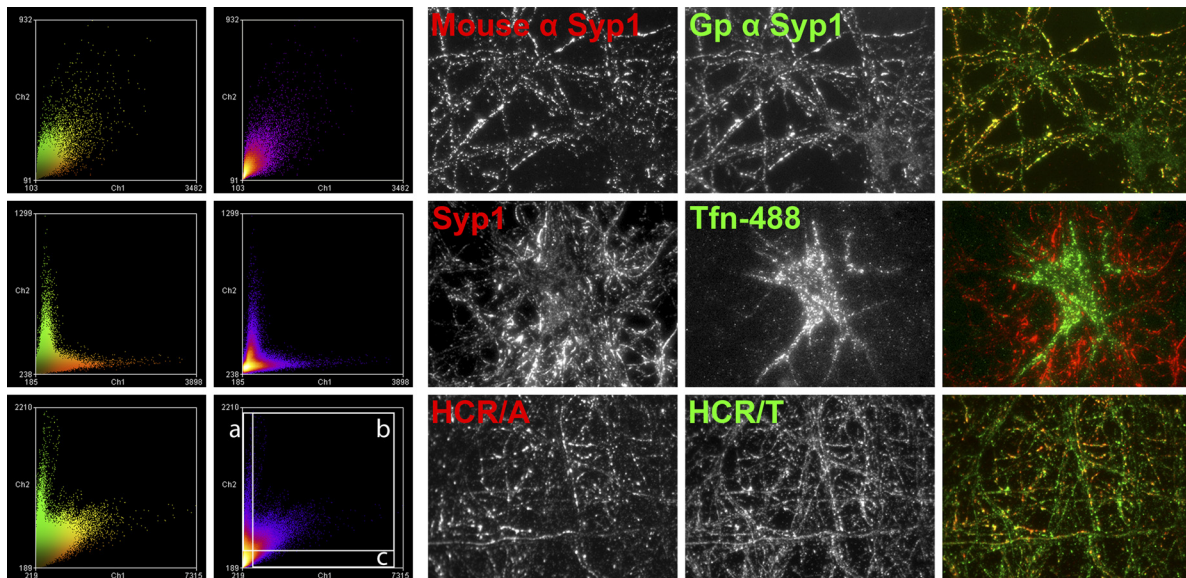
FIG 5 ImageJ analysis of HCR/T and HCR/A localization in primary neurons. Frequency scatterplots from ImageJ analysis were generated as the intensity of each pixel in one image plotted against the intensity of the same pixel in the second image. Neurons were stained with two species of antibody to synaptophysin 1 (top row, colocalized signals) (Gp, guinea pig), allowed to take up Alexa 488-labeled transferrin (Tfn-488) and stained for synaptophysin (middle row, segregated signals), and incubated with HA-HCR/A and FLAG-HCR/T and stained for the respective epitope (bottom row). Images are representative and had Pearson's coefficients of 0.756 (top row), 0.206 (middle row), and 0.600 (bottom row). The areas boxed in the bottom-row scatterplot are a representation of the threshold performed in a MetaMorph analysis for determining the percent colocalization between HCR/A and HCR/T in Fig. 4. (a) HCR/T positive and HCR/A negative; (b) HCR/T and HCR/A positive; (c) HCR/T negative and HCR/A positive. The column to the right of area a contains ~70% of the HCR/T signal, and area c contains ~30% of the HCR/A signal. The double positive population (b) contains ~30% of the HCR/T signal and ~70% of the HCR/A signal. The bottom-left box contains pixels that represent background signal.
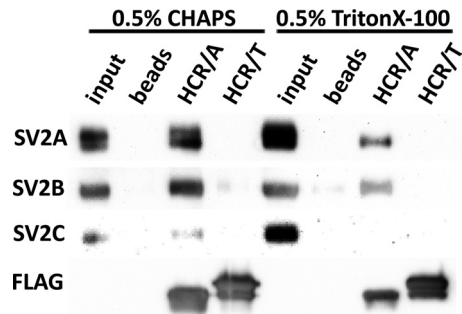
FIG 7 Differential binding of HCR/A and HCR/T to SV2. FLAG-HCR/A or FLAG-HCR/T (5 μg) was incubated with 10 μg of an SV cell lysate. Bound HCR was extracted with anti-FLAG agarose beads. HCRs were eluted with FLAG peptide, and eluted material was analyzed by Western blotting. Quantitation showed that in the CHAPS cell lysate SV2B bound to HCR/T was ~2% of SV2B bound to HCR/A.

HCR/T does not bind SV2. Synaptic vesicle protein 2 (SV2) is the protein receptor that targets BoNT/A to SVs (13). Experiments measured the direct binding of SV2 to FLAG-HCR/A and FLAG-HCR/T by immunoprecipitation. HCR-SV2 binding was measured in detergent-extracted SV lysates. HCR/A bound all three SV2 isotypes in CHAPS-solubilized lysates and bound SV2A and SV2B in Triton X-100-solubilized lysates. HCR/T did not bind detectable amounts of the SV2 isotypes in either detergent (Fig. 7). These experiments show that, within the limits of detection, HCR/T does not directly bind SV2.

Intoxication of neurons by TeNT. TeNT intoxication of depolarized, nondepolarized, and EGTA-treated neurons was also measured. TeNT efficiently cleaved VAMP2 under all conditions (Fig. 8). There was a small, but statistically significant, increase in VAMP2 cleavage in depolarized neurons relative to that in resting neurons, supporting entry of a subpopulation of TeNT into SVs upon membrane depolarization.

DISCUSSION

The current study shows that TeNT utilizes two entry pathways into neurons of the CNS. HCR/T entered neurons independent of stimulated synaptic vesicle cycling as well as via synaptic vesicle cycling. Colocalization analysis showed that most cell-associated HCR/T is segregated from HCR/A, with a subpopulation of HCR/T colocalized with HCR/A. Since HCR/T did not compete with HCR/A for entry into neurons and did not bind SV2, the protein receptor for BoNT/A, TeNT and BoNT/A enter SVs by independent mechanisms.

Endocytosis is essential for delivery of cargo between the plasma membrane and intracellular organelles (41). In neurons, intracellular trafficking is segregated, where SVs are present in the neuronal axon and transferrin receptor localizes in the soma and dendrites (reviewed in reference 6). Neurons utilize specialized endocytosis to rapidly cycle SV proteins on and off the plasma membrane. This involves multiple pathways to replenish SVs for neuronal signaling (8, 11, 32). In addition to direct cycling of SV proteins from the plasma membrane (42), an endosome-mediated pathway appears to recycle SV proteins from the plasma membrane (22). HCR/T entered neurons that were blocked for SV cycling, supporting the use of an endosome-mediated SV protein recycling pathway. An endosomal TeNT entry pathway has been described in motor neurons (12), and this pathway retrograde
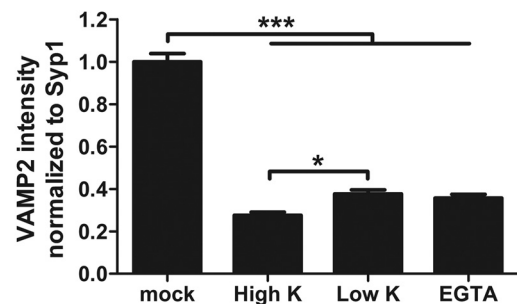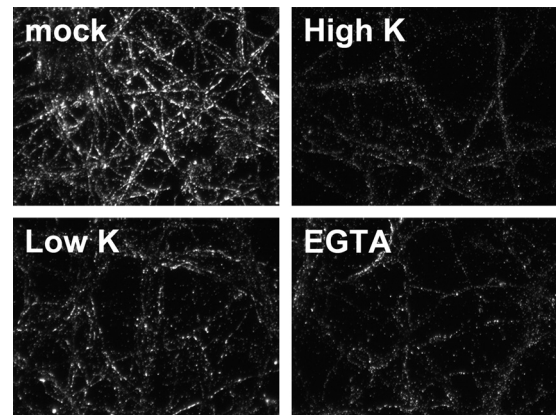
FIG 8 TeNT cleavage of VAMP2 in rat cortical neurons. Rat cortical neurons were incubated alone (mock) or with 20 nM TeNT in high K buffer (High K), low K buffer (Low K), or high K/EGTA buffer (EGTA) for 20 min at 37°C. Cells were washed and incubated in conditioned neurobasal medium for an additional 18 h. Cells were fixed and processed for VAMP2 content by IF. VAMP2 cleavage was assayed with mouse anti-VAMP2 antibody (1:500 dilution; SYSY clone 69.1), which recognizes only intact VAMP2. Data are representative of 5 random fields from two independent experiments. *, $P < 0.05$; ***, $P < 0.001$. Error bars indicate standard deviations.

traffics neurotrophin receptors TrkB and p75NTR, as well as poliovirus and canine adenovirus (reviewed in reference 34).

The organization of SV proteins into complexes was first described by Bennett and colleagues (2); in that study, SV protein complexes were detected following detergent solubilization. CHAPS solubilization preserved a large SV-protein complex composed of SV2, synaptophysin, synaptotagmin, VAMP2, and the proton vATPase, while Triton X-100 solubilization preserved only interactions between SV2-synaptotagmin and synaptophysin-VAMP2. Although the physiological function of these SV protein complexes remains unclear, interactions with SV complexes and BoNT HCRs have been observed (1). In the current study, HCR/A bound SV2 isoforms in detergent-solubilized SV lysates, while HCR/T did not bind any isoform of SV2, indicating that HCR/T does not bind SV2 directly or that the affinity was too low to detect under the assay conditions. An earlier study that reported the direct binding of TeNT to SV2 (43) did not normalize for immunoprecipitation efficiency, which may account for the differences in result. The current study supports entry of TeNT into neurons through the direct binding to dual gangliosides, rather than via SV2 binding (10), where TeNT binding and entry into gangliosides are necessary and sufficient in neurons and nonneuronal cells. Chen et al. (10) demonstrated that treatment of ganglioside-loaded PC12 cells, a pheochromocytoma cell line, with proteinase K does not change the cell association of HCR/T and that loading

HeLa cells with exogenous ganglioside is sufficient for HCR/T cell entry. A role for gangliosides in TeNT entry is also supported by earlier determinations that mice lacking complex gangliosides by disruption of GM2/GD2 synthase are ~600-fold more resistant to TeNT than wild-type mice (23).

Questions about TeNT entry into neurons remain. For example, are TeNT-ganglioside interactions on the cell membrane sufficient to initiate endocytosis? TeNT binding to dual gangliosides in the host plasma membrane may initiate endocytosis via membrane bending on the plasma membrane, as recently reported for viruses and toxins that bind multiple gangliosides as receptors (14, 31). Alternatively, an additional interaction on the cell membrane may be required to initiate endocytosis (18). Studies on TeNT entry are complicated by the two classes of neurons encountered during natural intoxication. By necessity, TeNT must traffic through motor neurons to enter and intoxicate inhibitory neurons in the CNS. This suggests that TeNT employs neuron-specific entry mechanisms. Earlier studies reported that high doses of TeNT elicit flaccid paralysis (15), which may represent entry of TeNT into peripheral motor neurons by an acidification-related pathway, possibly during SV cycling. In reciprocal experiments, high doses of BoNT/A elicit effects on the central nervous system (7). This suggests that BoNTs, like TeNT, can retrograde traffic through motor neurons. The specificity of the paralysis associated with botulism and tetanus may reflect the physiological amounts of toxin that are associated with natural infections. Continued studies on the mechanism(s) for the intracellular trafficking of the CNTs should enhance our understanding of intoxication and may identify new targets to extend the use of CNTs in human disease therapy.

ACKNOWLEDGMENTS

REFERENCES

1. **Baldwin MR, Barbieri JT.** 2007. Association of botulinum neurotoxin serotypes A and B with synaptic vesicle protein complexes. Biochemistry **46:**3200–3210.
2. **Bennett MK, Calakos N, Kreiner T, Scheller RH.** 1992. Synaptic vesicle membrane proteins interact to form a multimeric complex. J. Cell Biol. **116:**761–775.
3. **Binz T, et al.** 1994. Proteolysis of SNAP-25 by types E and A botulinal neurotoxins. J. Biol. Chem. **269:**1617–1620.
4. **Blasi J, et al.** 1993. Botulinum neurotoxin A selectively cleaves the synaptic protein SNAP-25. Nature **365:**160–163.
5. **Blasi J, et al.** 1993. Botulinum neurotoxin C1 blocks neurotransmitter release by means of cleaving HPC-1/syntaxin. EMBO J. **12:**4821–4828.
6. **Bonanomi D, Benfenati F, Valtorta F.** 2006. Protein sorting in the synaptic vesicle life cycle. Prog. Neurobiol. **80:**177–217.
7. **Caleo M, Schiavo G.** 2009. Central effects of tetanus and botulinum neurotoxins. Toxicon **54:**593–599.
8. **Chapman ER.** 2008. How does synaptotagmin trigger neurotransmitter release? Annu. Rev. Biochem. **77:**615–641.
9. **Chen C, Baldwin MR, Barbieri JT.** 2008. Molecular basis for tetanus toxin coreceptor interactions. Biochemistry **47:**7179–7186.
10. **Chen C, Fu Z, Kim J-JP, Barbieri JT, Baldwin MR.** 2009. Gangliosides as high affinity receptors for tetanus neurotoxin. J. Biol. Chem. **284:**26569–26577.
11. **Cousin MA.** 2000. Synaptic vesicle endocytosis: calcium works overtime in the nerve terminal. Mol. Neurobiol. **22:**115–128.
12. **Deinhardt K, Schiavo G.** 2005. Endocytosis and retrograde axonal traffic in motor neurons. Biochem. Soc. Symp. **72:**139–150.
13. **Dong M, et al.** 2006. SV2 is the protein receptor for botulinum neurotoxin A. Science **312:**592–596.
14. **Ewers H, et al.** 2010. GM1 structure determines SV40-induced membrane invagination and infection. Nat. Cell Biol. **12:**11–18.
15. **Fedinec AA, Toth P, Bizzini B.** 1985. Relation of spastic and flaccid paralysis to retrograde transport of 125I-tetanus toxin and its 125I-Ibc fragment. Modulating effect of F (ab) antibodies directed to specific areas on the toxin molecule. Boll. Ist. Sieroter. Milan. **64:**35–41.
16. **Fischer A, Mushrush DJ, Lacy DB, Montal M.** 2008. Botulinum neurotoxin devoid of receptor binding domain translocates active protease. PLoS Pathog. **4:**e1000245.
17. **Foran P, Lawrence GW, Shone CC, Foster KA, Dolly JO.** 1996. Botulinum neurotoxin C1 cleaves both syntaxin and SNAP-25 in intact and permeabilized chromaffin cells: correlation with its blockade of catecholamine release. Biochemistry **35:**2630–2636.
18. **Gil C, Chaib-Oukadour I, Aguilera J.** 2003. C-terminal fragment of tetanus toxin heavy chain activates Akt and MEK/ERK signalling pathways in a Trk receptor-dependent manner in cultured cortical neurons. Biochem. J. **373:**613–620.
19. **Gill DM.** 1982. Bacterial toxins: a table of lethal amounts. Microbiol. Rev. **46:**86–94.
20. **Habermann E, Dreyer F.** 1986. Clostridial neurotoxins: handling and action at the cellular and molecular level. Curr. Top. Microbiol. Immunol. **129:**93–179.
21. **Herreros J, Ng T, Schiavo G.** 2001. Lipid rafts act as specialized domains for tetanus toxin binding and internalization into neurons. Mol. Biol. Cell **12:**2947–2960.
22. **Hoopmann P, et al.** 2010. Endosomal sorting of readily releasable synaptic vesicles. Proc. Natl. Acad. Sci. U. S. A. **107:**19055–19060.
23. **Kitamura M, Takamiya K, Aizawa S, Furukawa K, Furukawa K.** 1999. Gangliosides are the binding substances in neural cells for tetanus and botulinum toxins in mice. Biochim. Biophys. Acta Mol. Cell Biol. Lipids **1441:**1–3.
24. **Lacy DB, Stevens RC.** 1999. Sequence homology and structural analysis of the clostridial neurotoxins. J. Mol. Biol. **291:**1091–1104.
25. **Matteoli M, et al.** 1996. Synaptic vesicle endocytosis mediates the entry of tetanus neurotoxin into hippocampal neurons. Proc. Natl. Acad. Sci. U. S. A. **93:**13310–13315.
26. **Montecucco C.** 1986. How do tetanus and botulinum toxins bind to neuronal membranes? Trends Biochem. Sci. **11:**314–317.
27. **Montecucco C, Schiavo G.** 1994. Mechanism of action of tetanus and botulinum neurotoxins. Mol. Microbiol. **13:**1–8.
28. **Montecucco C, Schiavo G.** 1995. Structure and function of tetanus and botulinum neurotoxins. Q. Rev. Biophys. **28:**423–472.
29. **Pellizzari R, Rossetto O, Schiavo G, Montecucco C.** 1999. Tetanus and botulinum neurotoxins: mechanism of action and therapeutic uses. Philos. Trans. R. Soc. Lond. B Biol. Sci. **354:**259–268.
30. **Poulain B.** 1994. Molecular mechanism of action of tetanus toxin and botulinum neurotoxins. Pathol. Biol. (Paris) **42:**173–182.
31. **Romer W, et al.** 2007. Shiga toxin induces tubular membrane invaginations for its uptake into cells. Nature **450:**670–675.
32. **Rosen LB, Ginty DD, Weber MJ, Greenberg ME.** 1994. Membrane depolarization and calcium influx stimulate MEK and MAP kinase via activation of Ras. Neuron **12:**1207–1221.
33. **Rummel A, et al.** 2009. Botulinum neurotoxins C, E and F bind gangliosides via a conserved binding site prior to stimulation-dependent uptake with botulinum neurotoxin F utilising the three isoforms of SV2 as second receptor. J. Neurochem. **110:**1942–1954.
34. **Salinas S, Schiavo G, Kremer EJ.** 2010. A hitchhiker's guide to the nervous system: the complex journey of viruses and toxins. Nat. Rev. Microbiol. **8:**645–655.
35. **Schiavo G, Matteoli M, Montecucco C.** 2000. Neurotoxins affecting neuroexocytosis. Physiol. Rev. **80:**717–766.
36. **Schiavo G, et al.** 1993. Identification of the nerve terminal targets of botulinum neurotoxin serotypes A, D, and E. J. Biol. Chem. **268:**23784–23787.
37. **Schiavo G, Rossetto O, Santucci A, DasGupta BR, Montecucco C.** 1992. Botulinum neurotoxins are zinc proteins. J. Biol. Chem. **267:**23479–23483.

38. **Schiavo G, et al.** 1993. Botulinum neurotoxins serotypes A and E cleave SNAP-25 at distinct COOH-terminal peptide bonds. FEBS Lett. **335:**99–103.

39. **Schwab M, Thoenen H.** 1977. Selective trans-synaptic migration of tetanus toxin after retrograde axonal transport in peripheral sympathetic nerves: a comparison with nerve growth factor. Brain Res. **122:**459–474.

40. **Schwab ME, Thoenen H.** 1978. Selective binding, uptake, and retrograde transport of tetanus toxin by nerve terminals in the rat iris. An electron microscope study using colloidal gold as a tracer. J. Cell Biol. **77:**1–13.

41. **Scita G, Di Fiore PP.** 2010. The endocytic matrix. Nature **463:**464–473.

42. **Sudhof TC.** 2004. The synaptic vesicle cycle. Annu. Rev. Neurosci. **27:**509–547.

43. **Yeh FL, et al.** 2010. SV2 mediates entry of tetanus neurotoxin into central neurons. PLoS Pathog. **6:**e1001207.